IEEE Photonics Journal
An IEEE Photonics Society Publication

Open Access

52 km-Long Transmission Link Using a 50 Gb/s *O*-Band Silicon Microring Modulator Co-Packaged With a 1V-CMOS Driver

Volume 11, Number 4, August 2019

Miltiadis Moralis-Pegios
Stelios Pitris
Theoni Alexoudi
Hannes Ramon
Xin Yin
Johan Bauwelinck
Yoojin Ban
Peter De Heyn
Joris Van Campenhout
Nikos Pleros

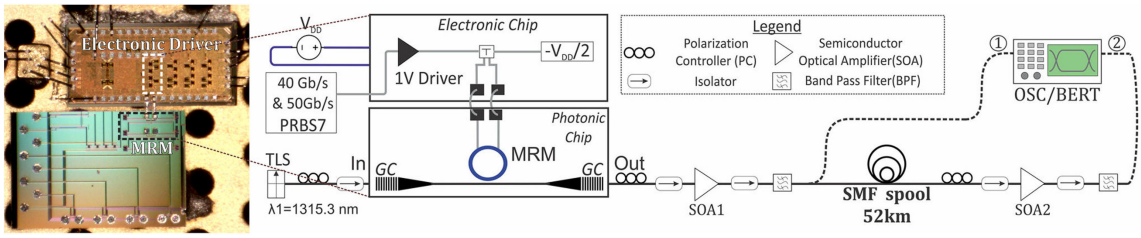

DOI: 10.1109/JPHOT.2019.2921730
1943-0655

52 km-Long Transmission Link Using a 50 Gb/s *O*-Band Silicon Microring Modulator Co-Packaged With a 1V-CMOS Driver

Miltiadis Moralis-Pegios,[1,2] **Stelios Pitris**,[1,2] **Theoni Alexoudi**,[1,2] **Hannes Ramon**,[3] **Xin Yin**,[3] **Johan Bauwelinck**,[3] **Yoojin Ban**,[4] **Peter De Heyn**,[4] **Joris Van Campenhout**,[4] **and Nikos Pleros**[1,2]

[1]Department of Informatics, Aristotle University of Thessaloniki, 54124, Thessaloniki, Greece
[2]Center for Interdisciplinary Research and Innovation, Aristotle University of Thessaloniki, 54124, Thessaloniki, Greece
[3]Department of Information Technology, IDLab, Ghent University imec, B-9052, Ghent, Belgium
[4]IMEC, B-3001 Leuven, Belgium

DOI:10.1109/JPHOT.2019.2921730

Manuscript received May 3, 2019; revised May 29, 2019; accepted June 4, 2019. Date of publication June 7, 2019; date of current version June 25, 2019. This work was supported in part by the European Commission H2020 Projects ICT-STREAMS (Contract 688172) and in part by the L3MATRIX (Contract 688544). Corresponding author: Miltiadis Moralis-Pegios (email: mmoralis@csd.auth.gr).

Abstract: We present an *O*-band silicon microring modulator with up to 50 Gb/s modulation rates, co-packaged with a 1V-CMOS driver in a dispersion un-compensated, transmission experiment through 52 km of standard single-mode fiber. The experimental results show 10^{-9} error-rate operation with a negligible power penalty of 0.2 dB for 40 Gb/s and wide-open eye diagrams for 50 Gb/s data, corresponding to a record high bandwidth-distance product of 2600 Gb·km/s. A comparative analysis between the proposed transmitter assembly and a commercial $LiNbO_3$ modulator revealed a moderate increase of 3.8 dB in power penalty, requiring only 20% of the driving voltage level used by the commercial modulator.

Index Terms: Optical interconnects, silicon microring modulator, optical transmission.

1. Introduction

The on-going transition to 5G standards combined with the imminent proliferation of Internet of Thing (IoT) devices and the exponential growth of data center (DC) traffic [1] is calling for advances in optical transceiver technologies that eventually have to meet the diverse requirements extending from chip-to-chip and data center network interconnections [2] up to high-speed data transmission links in telecom applications. Silicon photonics (SiP) emerge as a promising transceiver technology across the complete chain of interconnect hierarchy, offering a number of important advantages: i) compatibility with existing CMOS processes and strong volume-manufacturing potential [3], ii) capability of co-integration with advanced microelectronics [4] and iii) low power consumption [3]–[5]. Among SiP devices, the micro-ring modulator (MRM) appears as a key component due to its

ultra-low footprint, high-bandwidth [5] and inherent compatibility with wavelength division multiplexed (WDM) systems [6], [7]. So far, the majority of the already proposed MRM designs [3], [8], [9] have targeted operation in the C-band to exploit the lower standard single mode fiber (SSMF) losses and the availability of low noise EDFA-based amplification. However, the frequency chirp of conventional MRM designs [10] and the strong chromatic dispersion (CD) of SSMF in the C-band are limiting the maximum extent of the transmission link [11], necessitating dispersion compensation schemes for increasing the transmission reach. To this end, sophisticated yet complex, low-chirp MRM designs have been proposed for enabling high transmission distances in dispersion uncompensated fiber links [12], achieving a bandwidth-distance product of 800 Gb-km/sec when transmitting 40 Gb/s data over 20 km long fiber link, and 1000 Gb-km/sec when transmitting 12.5 Gb/s data over an 80 km long fiber link [13].

On the other hand, O-band MRMs [5], [14], [15] can leverage the very low CD of SSMF in this spectral region to allow much higher transmission distances without dispersion compensation, with prior demonstrations of 40 Gb/s data transmission over 40 km-long fiber links setting the record-value of the bandwidth-distance product at 1600 Gb-km/s [14]. However, this record-value has been accomplished by O-band silicon MRM designs that require relatively high (3-4 V_{p-p}) driving voltages [14], suggesting significant challenges for the required high-speed electronic driver circuitry, especially when high bandwidth-distance product together with low-energy consumption at the transmitter side are targeted. Reduced energy consumption has been recently accomplished by employing a high-speed inverter-based CMOS driver with only 1 Vpp output in a co-packaged SiP transmitter module driving a high-speed, low voltage C-band silicon MRM [16] and demonstrating 56 Gb/s operation over 2 km with a power consumption as low as 0.71 pJ/bit. Transferring these credentials to O-band designs [17] can offer compact and energy-efficient SiP transmitter assemblies that could eventually allow for high bandwidth-distance products in dispersion uncompensated links, being suitable for metro network optical communications.

In this paper, we report for the first time, to the best of our knowledge, a co-packaged O-band 50 Gbps silicon MRM-based transmitter using a high-speed inverter-based CMOS driver and demonstrate a record-high bandwidth distance product of 2600 Gb-km/s without employing dispersion compensation. The transmitter layout utilizes a 1V-CMOS driver wire-bonded to a silicon MRM and has been experimentally evaluated for 40 Gb/s and 50 Gb/s NRZ-OOK data signals, revealing 4.2 dB and 4.1 dB extinction ratios (ER) respectively, for an insertion loss value of 6 dB. The co-packaged driver module can operate from an input electrical data signal of only 75 mVpp and presents a power consumption of 40 mW, corresponding to an energy efficiency of 1 pJ/bit and 0.8 pj/bit, at 40 Gb/s and 50 Gb/s, respectively. Transmission of 40 Gb/s NRZ data, at 10^{-9} error-rate, with a negligible power penalty of 0.2 dB and open eye diagrams of 50 Gb/s NRZ data in a 52 km SSMF transmission link are reported, concluding to a 44% higher distance-bandwidth product compared to state-of-the-art literature demonstrations [14]. Finally, a comparative analysis between the MRMs-based transmitter and a commercial $LiNbO_3$ modulator paired with a 5 V driver is performed for 40 Gb/s NRZ data, revealing a moderate power penalty of 3.8 dB for the proposed MRM assembly, even though the electrical driving voltage of the commercial modulator was five-times higher.

2. The O-Band Silicon Microring Modulator and 1V-CMOS Driver Transmitter Package

A close-up view of the assembled MRM-based O-band transmitter is illustrated in Fig. 1(a). The transmitter comprises a photonic chip, fabricated in imec's ISSIPP50G platform, incorporating a high-speed carrier-depletion O-band MRM [5], which is wire bonded to a low-power 28-nm fully depleted Silicon-on-insulator (FD-SOI) electronic driver that is identical to the one reported in [16].

Figure 1(b) illustrates the mask layout of the MRM transmitter section on the photonic chip, comprising the high-speed RF MRM's pads along with two optical paths formed between respective input/output GCs: one path is a simple straight section and acts as the reference silicon branch,

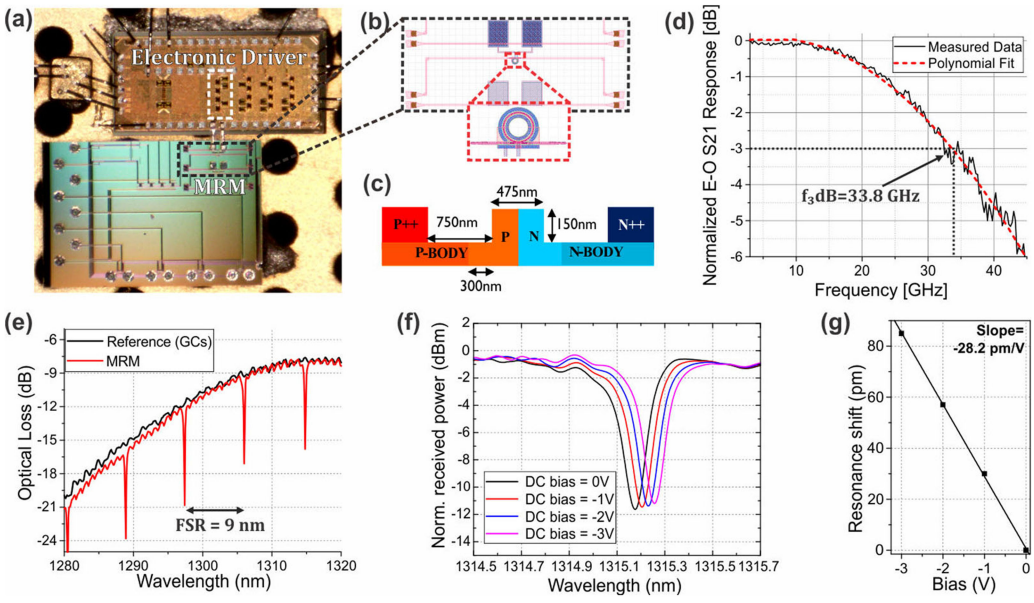

Fig. 1. (a) Close up view of the assembled O-band transmitter with the MRM wire bonded to the low power 1V-CMOS driver (b) Mask highlight of the MRM (c) Cross-section of the PN junction (d) MRM Electro-optic S21 response (e) Transmission spectra of the reference section and the MRM (f) Optical spectra of the MRM with 0 – (-3V) junction bias voltage (g) Fitted resonance wavelength shift of the MRM versus junction bias.

while the second silicon waveguide path incorporates the 7.5 μm radius MRM and is depicted in more detail in the zoomed-in inset. The MRM [5] is an all-pass ring embedded in a highly doped lateral PN junction, with a total length of 47.1 um, spanning through the whole circumference of the ring. A cross-section of the employed PN junction is shown in Fig. 1(c), illustrating the partly etched (150 nm) Si waveguide offering low series resistance and high guiding capability, along with other critical design dimensions of the employed junction. The MRM's Q factor was measured to be ~5000, close to the design specifications, resulting in a photon lifetime of approximately 3.5 ps at 1315 nm, while the simulated group index was 4.03 corresponding to an FSR of 9.0 nm. Calculation of the MRM 3-dB bandwidth was performed using the simplified model described in [3], where the cavity photon lifetime and the RC time delay act as low pass filters. As such, the cut-off frequency of the MRM was calculated at 34.9 Ghz, with the individual contributors corresponding to photon lifetime and RC time delay being $f_Q = 45.9$ GHz and $f_{RC} = 53.9$ GHz. Fig. 1(d) illustrates the normalized E-O S21 response, acquired at the point of maximum optical modulation amplitude (OMA) at approximately 1315 nm, revealing an f3dB of approximately 33.8 Ghz, closely matching the calculated 3-dB bandwidth.

The electronic and photonic chip were placed in close proximity, in order to minimize the wire bonding induced inductance, while the power and ground supply pins of the electronic driver were wire bonded to a general-purpose PCB and were accessible through input/output header pins. The electronic driver input was accessible through RF pads, while TE grating couplers (GCs) were used to couple light in and out of the photonic chip. Light from a tunable laser source (TLS) was launched into the chip through the TE GCs, in order to characterize both the reference and the MRM section, while light coupled from the output GCs to an optical fiber was measured by means of a high-precision optical power meter. Before launching the light to the chip, a polarization controller (PC) was employed, to match the incoming light's polarization to the input grating coupler. The optical transmission spectrum obtained at the MRM output is illustrated in Fig. 1(e). Based on the measurement of the straight reference branch section, the two grating couplers induced a minimum loss of 8 dB at 1315 nm. The MRM has a low single-pass loss of approximately 0.2 $\pm$ 0.2 dB at 1315 nm that is also the GC peak wavelength, caused by the scattering and absorption in the

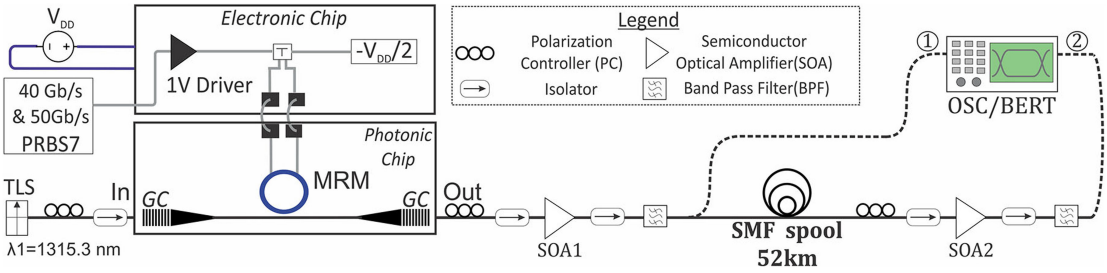

Fig. 2. Experimental Setup for characterization of the MRM-based transmitter in a 52 km optical transmission link.

doped region. The free spectral range (FSR) was measured to be 8.9 $\pm$ 0.1 nm, closely matching the design specifications, and the extinction ratio (ER) was at least 10 dB. By applying reverse voltage bias to the junction, the resonance of the MRM shifts as depicted in Fig. 1(d). The linear fitting of the values of the wavelength shift versus the applied negative voltage revealed an efficiency of 28.2 pm/V, as illustrated in Fig. 1(e).

3. Experimental Evaluation of 40 Gb/s and 50 Gb/s Data Transmission in a 52 km-Long Fiber Link

In order to assess the long-haul and high-speed credentials of the MRM-based transmitter, its performance was experimentally investigated with 40 Gb/s and 50 Gb/s OOK-NRZ data, in a 52 km-long transmission experiment.

The employed experimental setup is illustrated in Fig. 2. An RF-source was used to generate a NRZ pseudo-random binary sequence (PRBS7) at 40 Gb/s and 50 Gb/s, with a peak-amplitude of 307 mV, that was applied to the driver circuit through a high-speed RF probe. The electronic driver circuit was powered by a 1.1 V supply voltage (V_{DD}), applied at the PCB header pins. This value was slightly higher than the nominal 1 V to compensate for the PCB electrical routing losses. The driver's 1 Vp-p RF output was combined with a negative voltage of -V_{DD}/2, used for biasing the micro ring modulator at -0.5 V, and the resulting signal was applied to the MRM high frequency pads through wire bonds. A CW signal from a TLS at $\lambda_1 = 1315.3$ nm, close to the MRM's resonance, was launched into the photonic chip through a TE grating coupler, while a PC was used to match the incoming light's polarization to the grating coupler. It should be noted, that employment of an integrated heater structure for the MRM, already developed and demonstrated in [7], would allow higher flexibility in terms of operational wavelength. The resulting modulated signal was then coupled out of the chip through an output TE grating coupler and collected in a fiber. Injected input power was 10 dBm. With the two grating couplers inducing 8 dB losses at 1315 nm and the RM insertion losses being $\sim$6.2 dB, the optical signal obtained at the chip's output had an average power of -5.8 dBm. It should be noted, that given that the modulated signal has an ER of 4.2 dB and 50% duty cycle, the average power of -5.8 dBm at the MRR output corresponds to a peak optical power of -4.2 dBm. After exiting the silicon chip, the optical signal was launched into a 52 km standard single mode fiber (SSMF) link that had a dispersion of approximately -0.21 ps/nm$*$km at 1315.3 nm and a total loss of 17.4 dB, implying a propagation loss factor of 0.33 dB/km excluding the connector induced losses. The dispersion of the SSMF at the operational wavelength of $\lambda = 1315.3$ nm was estimated using the formula $D(\lambda) = \frac{s_0}{4}[\lambda - \frac{\lambda_0^4}{\lambda^3}]$ [18], with a zero-dispersion wavelength $\lambda_0 = 1317.7$ nm and a dispersion slope $s_0 = 0.088$ ps/nm^{2*}km at λ_0, obtained from the manufacturer specifications. In order to satisfy the power budget requirements, two SOAs (SOA1-SOA2) were employed before and after the SSMF spool to compensate for the chip insertion losses and the SSMF propagation losses. Isolators at the input and output of both SOAs were utilized to ensure unidirectional signal transmission inside the SOAs, while Optical Band Pass Filters (OBPFs) with a 2.5 nm bandwidth were used at the SOA outputs to filter out the SOA amplified spontaneous

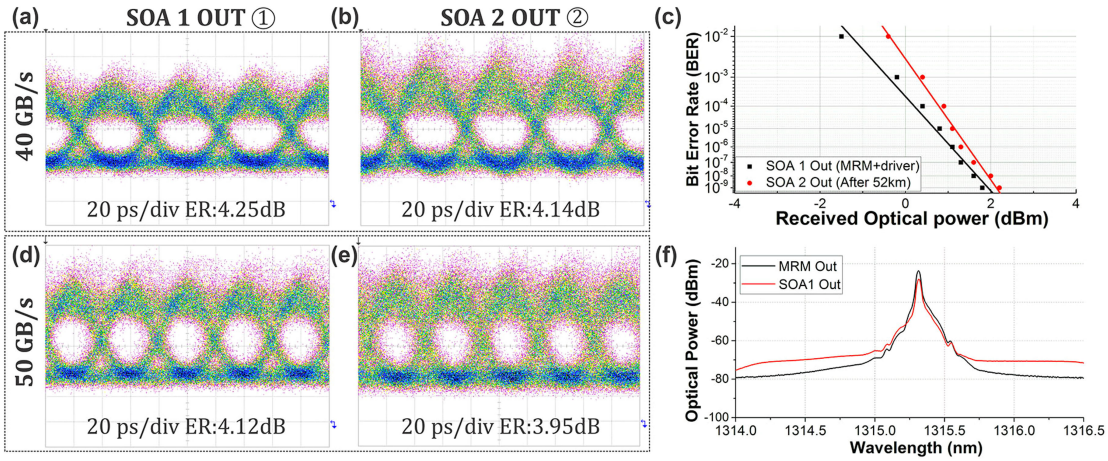

Fig. 3. (a), (b) Optical Eye diagram at SOA1 and SOA 2 Output at 40 Gb/s (c) BER measurements at 40 Gb/s, (d), (e) Optical Eye diagram at SOA1 and SOA 2 Output at 50 Gb/s (f) Optical Spectra at the MRM and SOA 1Output.

emission (ASE). Finally, PCs were utilized prior to the SOAs inputs to optimize the incoming light's polarization.

The optical signal was monitored at a sampling scope and evaluated by means of a BER tester at different points of the experimental setup, with the obtained results illustrated in Fig. 3. Fig. 3(a) depicts the optical eye diagram of the 40 Gb/s signal obtained at SOA1 output, revealing an open eye diagram with an ER of 4.25 dB for a low driving voltage of 1 V. The signal was then injected into the 52 km SSMF spool, amplified in SOA2 and filtered in a 2.5 nm bandwidth OBPF. Fig. 3(b) illustrates the obtained optical eye diagram at SOA2 Output, revealing a slightly decreased ER value of 4.14 dB. The obtained BER measurements at both SOA1 and SOA2 outputs are depicted in Fig. 3(c), revealing error-free operation for both cases, with an induced power penalty before and after the 52 km spool of $\sim$0.2 dB, at 10^{-9} error-rate. The same procedure was followed, when the MRM-based transmitter was operated at 50 Gb/s. Although no BER measurements could be carried out due to bandwidth limitations of the available BER Testing equipment, a high-quality signal was obtained both before and after the 52 km fiber link was obtained, as can be revealed by the clearly open eye diagrams with ER values of 4.12 dB and 3.95 dB at SOA1 and SOA2 Outputs shown in Fig. 3(d) and (e), respectively. Finally, Fig. 3(f) illustrates the optical spectra of the modulated signal at the MRM and SOA1 output, revealing a slightly increased noise floor originating from the SOA-induced ASE. SOA1 was operated at 280 mA offering a 15.8 dB gain at 1315 nm, while SOA2 was driven at 144 mA providing a gain of $\sim$14.8 dB. The power consumption of the co-packaged electronic driver was 40 mW, resulting to an energy efficiency of only 1 pJ/bit for 40 Gb/s and 0.8 pJ/bit for 50 Gb/s operation.

4. Comparative Analysis With a LiNbO3 Modulator

After validating the credentials of the MRM-based transmitter in long-reach applications, we evaluated its performance compared to a commercial O-band MZM-based 40 Gb/s $LiNbO_3$ modulator, paired with a suitable 5 V electronic driver. Fig. 4 depicts the experimental setup employed, comprising two separate data generation stages that were used inter-changeably in the setup. On the first stage, denoted (i) in Fig. 4, the MRM-modulator co-packaged with the 1V-driver was utilized, while the second stage, denoted (ii), employed a commercially available 40 Gb/s $LiNb0_3$ optical modulator driven by a 5 V electronic driver. In both cases, a 40 Gb/s $PRBS^7$-1 data signal with a peak amplitude of 307 mV, was applied to the respective electronic driver, while an optical beam

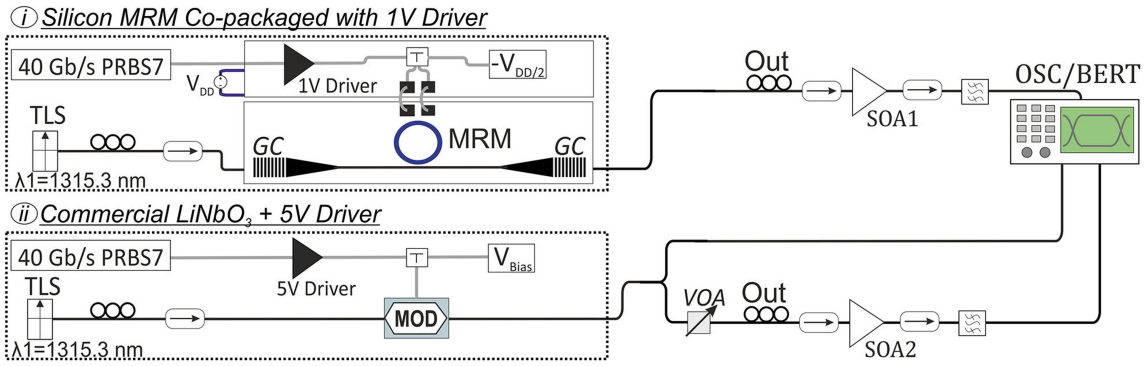

Fig. 4. Experimental Setup for the comparison of the MRM with a commercially available LiNbO3 modulator.

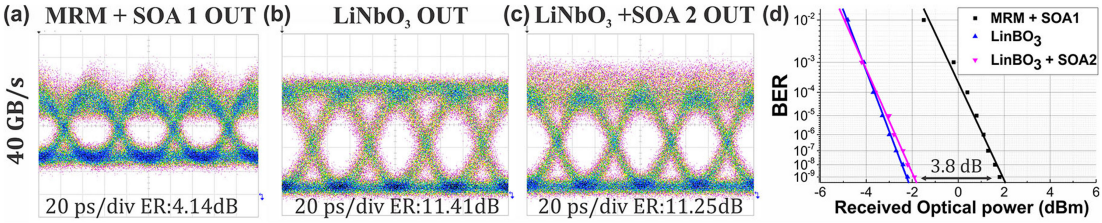

Fig. 5. (a) Optical Eye diagram at MRM+ SOA 1 Output, (b) Optical Eye diagram at $LiNbO_3$ Output, (c) Optical Eye diagram at $LiNbO_3$+ SOA 2 Output, (d) BER measurements.

generated from a TLS at $\lambda_1 = 1315.3$ nm with 10 dBm average optical power, was injected to the respective optical modulator. The modulated signal originating from the first data generation stage with the MRM was subsequently injected in SOA1 to compensate for both the coupling and insertion losses of the MRM chip that were 8 dB and 6 dB, respectively. SOA1 was preceded and followed by optical isolators to ensure unidirectional signal transmission, while the input polarization was optimized through a PC. After filtering in a 2.5 nm bandwidth OBPF, the optical signal was finally monitored at a sampling scope and evaluated via a BER tester. For the second data generation stage, a $LiNbO_3$ modulator was employed and two different scenarios were investigated: in the first scenario, the modulator output was directly evaluated via a BER tester and at a sampling scope, while in the second scenario the modulator output was injected in a variable optical attenuator (VOA) and was subsequently amplified in SOA2 prior being filtered in a OBPF and monitored. The VOA was employed to ensure equal optical power levels between the signals generated by the MRM- and LiNbO3-based modulation stages at the SOA1 and SOA 2 inputs, taking into account the different insertion losses of the MRM-chip and the $LiNbO_3$ stages that were 14 dB and 4 dB, respectively. Following the above methodology and since both of the SOAs employed were identical and operated in the same current (280 mA), it was feasible to perform a direct comparison between the two modulation approaches, quantifying also the signal degradation originating from the SOA amplification stages.

Figure 5 (a) depicts the obtained optical eye diagram of the 40 Gb/s signal at SOA1 Output, when the MRM-based transmitter and SOA1 are employed, revealing a clearly open eye diagram with an ER of 4.14 dB. Fig. 5(b) and (c) depict the 40 Gb/s optical eye diagrams, when the LiNbO3 modulator along with its 5 V driver are utilized, without and with the SOA2 amplification stage, revealing ERs of 11.41 dB and 11.25 dB, respectively. Fig. 5(d) illustrates the obtained BER measurements for all three cases. Considering the LiNbO3-based scenario, a negligible power-penalty of 0.2 dB, at 10^{-9} error rate, is reported when incorporating SOA2 in the optical link, revealing only low signal quality degradation due to amplification. Finally, for the MRM-based scenario, an increase of the power penalty of 3.8 dB at a 10^{-9} error rate was observed when compared to the amplified $LiNbO_3$ case, despite the five-fold difference in driving voltage.

4. Conclusion

A co-packaged 40 Gb/s O-band silicon transmitter with a record-high bandwidth-distance product of 2600 Gb-km/s has been reported, comprising a high-speed O-band MRM wire-bonded to a low-power 1V-CMOS electronic driver. The driver used 40 Gb/s and 50 Gb/s NRZ PRBS^7-1 input signals of 307 mV to drive the MRM with a Vp-p voltage of 1 V, producing optical signals with 4.25 dB and 4.14 dB ERs respectively, for an insertion loss of 6 dB. The signals at the MRM output are transmitted through 52 km of SSMF, and the BER measurements reveal a power penalty of $<$0.2 dB, at 10–9 error rate, for the 40 Gb/s case and open eye-diagrams for the 50 Gb/s case. Finally, a comparative analysis of the MRM-based transmitter versus a commercial $LiNbO_3$ modulator was performed, with the commercial modulator driven by a 5 V electronic driver. The analysis revealed a power penalty equal to 3.8 dB for the MRM assembly although the commercial modulator is operated with five-times higher driving voltage.

References

[1] "Cisco global cloud index: Forecast and methodology, 2015–2020," Cisco, White Paper, 2015.
[2] N. Terzenidis *et al.*, "High-port low-latency optical switch architecture with optical feed-forward buffering for 256-node disaggregated data centers," *Opt. Exp.*, vol. 26, pp. 8756–8766, 2018.
[3] M. Pantouvaki *et al.*, "Active components for 50 Gb/s NRZ-OOK optical interconnects in a silicon photonics platform," *J. Light. Technol.*, vol. 35, no. 4, pp. 631–638, Feb. 2017.
[4] A.H. Atabaki *et al.*, "Monolithic optical transceivers in 65 nm bulk CMOS," *Opt. Fiber Commun. Conf.*, vol. 1, 2018, Paper W1I.4.
[5] J. Van Campenhout *et al.*, "Silicon photonics for 56G NRZ optical interconnects," *Opt. Fiber Commun. Conf.*, 2018, Paper W1I.1.
[6] Q. Xu, B. Schmidt, J. Shakya, and M. Lipson, "Cascaded silicon micro-ring modulators for WDM optical interconnection," *Opt. Exp.*, vol. 14, pp. 9431–9435, 2006.
[7] S. Pitris *et al.*, "A 4×40 Gb/s O-band WDM silicon photonic transmitter based on micro-ring modulators," in *Proc. Opt. Fiber Commun. Conf. OSA Tech. Dig.*, 2019, Paper W3E.2.
[8] X. Xiao *et al.*, "High-speed silicon microring modulator based on zigzag PN junction," in *Proc. IEEE Photon. Conf.*, vol. 24, pp 256–257, 2012.
[9] G. Li *et al.*, "25Gb/s 1V-driving CMOS ring modulator with integrated thermal tuning," *Opt. Exp.*, vol. 19, pp. 20435–20443, 2011.
[10] L. Zhang *et al.*, "Microring-based modulation and demodulation of DPSK signal," *Opt. Exp.*, vol. 15, pp. 11564–11569, 2007.
[11] G. P. Agrawal, *Fiber-Optic Communication Systems*, 4th Ed. Hoboken, NJ, USA: Wiley, 2011.
[12] R. Li *et al.*, "High-speed low-chirp PAM-4 transmission based on push-pull silicon photonic microring modulators," *Opt. Exp.*, vol. 25, pp. 13222–13229, 2017.
[13] A. Biberman *et al.*, "First demonstration of long-haul transmission using silicon microring modulators," *Opt. Exp.*, vol. 18, pp. 15544–15452, 2010.
[14] Z. Xuan *et al.*, "Silicon microring modulator for 40 Gb/s NRZ-OOK metro networks in O-band," *Opt. Exp.*, vol. 22, pp. 28284–28291, 2014.
[15] H. Li *et al.*, "A 112 Gb/s PAM4 Transmitter with Silicon Photonics Microring Modulator and CMOS Driver," in *Proc. Opt. Fiber Commun. Conf.*, 2019, Paper Th4A.4.
[16] H. Ramon *et al.*, "Low-power 56Gb/s NRZ microring modulator driver in 28 nm FDSOI CMOS," *IEEE Photon. Technol. Lett.*, vol. 30, no. 5, pp. 467–470, Mar. 2018.
[17] S. Pitris *et al.*, "A 40 Gb/s chip-to-chip interconnect for 8-socket direct connectivity using integrated photonics," *IEEE Photon. J.*, vol. 10, no. 5, Oct. 2018. Art. no. 6601808.
[18] Corning SMF-28e Optical Fiber Product Information, 2007. [Online]. Available: http://www.princetel.com/datasheets/smf28e.pdf